J Mater Sci (2010) 45:5814–5819
DOI 10.1007/s10853-010-4656-4

Facile fabrication of nano-hydroxyapatite/silk fibroin composite via a simplified coprecipitation route

Chunquan Fan · Jiashun Li · Guohua Xu · Hailong He · Xiaojian Ye · Yuyun Chen · Xiaohai Sheng · Jianwei Fu · Dannong He

Received: 11 August 2009 / Accepted: 9 November 2009 / Published online: 8 June 2010
© Springer Science+Business Media, LLC 2010

Abstract Nano-hydroxyapatite/silk fibroin (n-HA/SF) composite was successfully fabricated based on a simplified coprecipitation route. In detail, the degummed SF was first dissolved in $CaCl_2$ aqueous/ethanol solution without desalting procedure, and then $(NH_4)_2HPO_4$ solution and NH_4OH were dropped into the above solution to form n-HA/SF composite. The structure and morphology of n-HA/SF composite were investigated by Transmission electron microscopy, Fourier transform infrared spectrometry, energy dispersive X-Ray spectrum, X-ray diffraction, and thermogravimetric analyses. Results indicate that the inorganic phase is carbonate-substituted HA with low crystallinity and similar to the crystals of human bone. The HA crystals have diameter of around 20–30 nm and length of about 200–500 nm. The content of SF in the composite is about 30%, and the two phases bonded each other strongly. In addition, a formation mechanism of n-HA/SF was proposed.

Introduction

Natural bone is a complex inorganic/organic nanocomposite material, in which about 70 wt% hydroxyapatite (HA) nanocrystals and about 30 wt% collagen fibrils are well organized into hierarchical architecture over several length scales [1, 2]. The HA/collagen nanocomposites for artificial bones have been developed by biomimetic processing, which was based on the idea that biologic systems store and process information at the molecular level [3–5]. This kind of nanocomposites could mimic the nanostructure of real bone and display remarkable physical and chemical features. However, due to some practical problems with collagen, high cost, difficulty to control cross-infection, and the poor definition of commercial sources [6], there is a need to explore new synthetic or natural organic materials instead of collagen for the development of biomimetic bone materials.

Currently, some biocompatible polymers or proteins, such as chitosan [7–9], alginate [10], polylactic acid [11], poly-lactic-glycolic acid [12], polyamide [13], hyaluronic acid [14], and silk fibroin [15–17], have been reported to combine with HA. Among them, silk fibroin (SF) is of practical interest due to its excellent intrinsic properties utilizable in the biotechnological and biomedical fields. SF, a hard protein extract from silk cocoons, is composed of 17 amino acids. SF has been proved to be good biocompatible material and has been successfully used for various medical applications. It was demonstrated that silk fibers could induce apatite deposition on the surfaces of proteins in solution mimicking body fluid [18]. For this reason, a coprecipitation method was often used to synthesize silk powder/HA nanocomposites [15, 16, 19]. As-synthesized nanocomposites could take on outstanding osteoconductivity and bioactivity and display huge potential as biomaterials for a series of different applications. However, the conventional coprecipitation route for preparing HA/SF composite comprises a desalting procedure (dialysis), which usually at least expends 3 days. Moreover, a thorough understanding of the process of apatite formation on the silk fiber is far from understood.

C. Fan · J. Li · G. Xu · H. He · X. Ye (✉)
Department of Orthopedic Surgery, Changzheng Hospital, Second Military Medical University, 415 Fengyang Road, Shanghai 200003, People's Republic of China
e-mail: yexj2002@yahoo.com.cn

Y. Chen · X. Sheng · J. Fu · D. He
National Engineering Research Center for Nanotechnology, Shanghai 200241, People's Republic of China

In the present study, we tried to put forward a simplified coprecipitation route to n-HA/SF composite in order to be time-saving and efficient. In details, the *Bombyx mori* silk fibers after degumming sericin were directly dissolved in $CaCl_2$ aqueous/ethanol solution without desalting procedure, and then $(NH_4)_2HPO_4$ solution and NH_4OH were added dropwise into the above solution to form n-HA/SF composite. Meanwhile, the formation mechanism of the composite was proposed on the basis of analyzing the chemical interaction between SF and HA.

Experimental

Na_2CO_3, $CaCl_2$, CH_3CH_2OH, NH_4OH, and $(NH_4)_2HPO_4$ used here are OF analytical grade and purchased from Shanghai Chemical Reagents Corp. (Shanghai, China). *Bombyx mori* silkworm cocoons were obtained from Huzhou Academy of Agricultural Science (Huzhou, China).

Bombyx mori silkworm cocoons were boiled for 30 min in an aqueous solution of 0.5% (w/v) Na_2CO_3 and were then thoroughly washed with distilled water to extract the glue-like sericin proteins. The treatment was repeated three times to obtain the pure SF. The degummed SF was vacuum-dried at 80 °C for 24 h.

With the inorganic/organic weight ratio (70/30) as a guideline, the weight ratio of HA/SF in the final product aim to be 70/30. The molar ratio of Ca/P in the starting mixture was set as 1.67, equal to that of stoichiometric HA. 4.30 g dried degummed SF was first dissolved in an aqueous/ethanol solution containing 11.10 g $CaCl_2$ ($CaCl_2$:CH_3CH_2OH:H_2O = 1:2:8, molar ratio) at 75 °C for about 30 min, and then 120 ml 0.5 M $(NH_4)_2HPO_4$ solution was added dropwise into above solution. The solution was titrated with ammonium hydroxide in drops to maintain the pH at 10.0. The reaction temperature was kept at 75 °C and the solution was stirred at 800 rpm for 3 h, followed by 24 h of aging at ambient temperature. Afterwards, three cycles of alternate centrifugation and water-washing were carried out to harvest the precipitates. The resulting precipitates were dried under vacuum at 50 °C for 24 h to yield n-HA/SF composite. Meanwhile, pure HA without SF was prepared as a control sample by the same procedure. The whole preparation process can be schematically illustrated in Fig. 1.

The FT-IR measurements were conducted on a Perkin-Elmer Paragon 1000 Fourier transform spectrometer at room temperature (25 °C). The samples were mixed with KBr pellets to press into the small flakes. Transmission electron microscopy (TEM) and energy dispersive X-Ray spectrum (EDS) were performed with a JEOL JEM-100CX microscope operated at 100 kV. Samples for TEM were diluted 50 times with anhydrous alcohol and then dropped on copper grids and allowed to dry under infrared lamp. The X-ray diffraction (XRD) pattern was recorded on a powder sample using X-ray diffractometer (D/MAX-2200PC, CuKa radiation, Japan). The samples were scanned from 20° to 60° with a scanning rate of 4° min^{-1}. Thermogravimetric analyses (TGA) were performed on a Perkin Elmer TGA 7/DX thermogravimetric analyzer (TA instruments) in the temperature range from ambient temperature to 800 °C at a heating rate of 10 °C·min^{-1} under air atmosphere at a flow of 100 mL min^{-1}. The thermal degradation temperature was taken as the onset temperature at which 5 wt% of weight loss occurs.

Results and discussion

Figure 2a–d shows the typical TEM images of HA and the n-HA/SF composite. There is a distinct difference in shape between them. The former is rod-like in shape with a typical size of about 200 nm in length and about 50 nm in width, while the latter is the bundle of nanofibrils with the size of 200–500 nm in length and 20–30 nm in width. The ED pattern (Fig. 2e) from the n-HA/SF composite displays polycrystalline rings, which are well indexed as the HA phase with (002) preferential orientations [6]. It is well known that the HA nanocrystals in bone have a preferred (002) crystallographic orientation owing to the *c*-axis of the crystals that are approximately parallel to the long axis direction of SF. Figure 2f is a typical energy dispersive X-Ray spectrum taken from a composite area. C, O, P, and Ca peaks are present in the spectrum, indicating that the composite is composed of HA and SF. Meanwhile, EDS area analysis of the composite reveals a Ca/P (7.47/4.5 = 1.66) molar ratio similar to that of pure HA

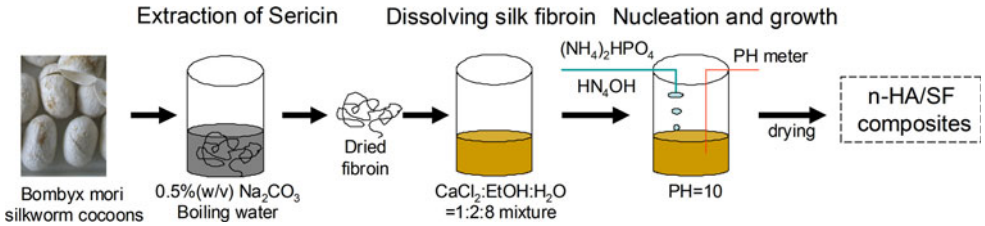

Fig. 1 Procedure for the fabrication of n-HA/SF composite

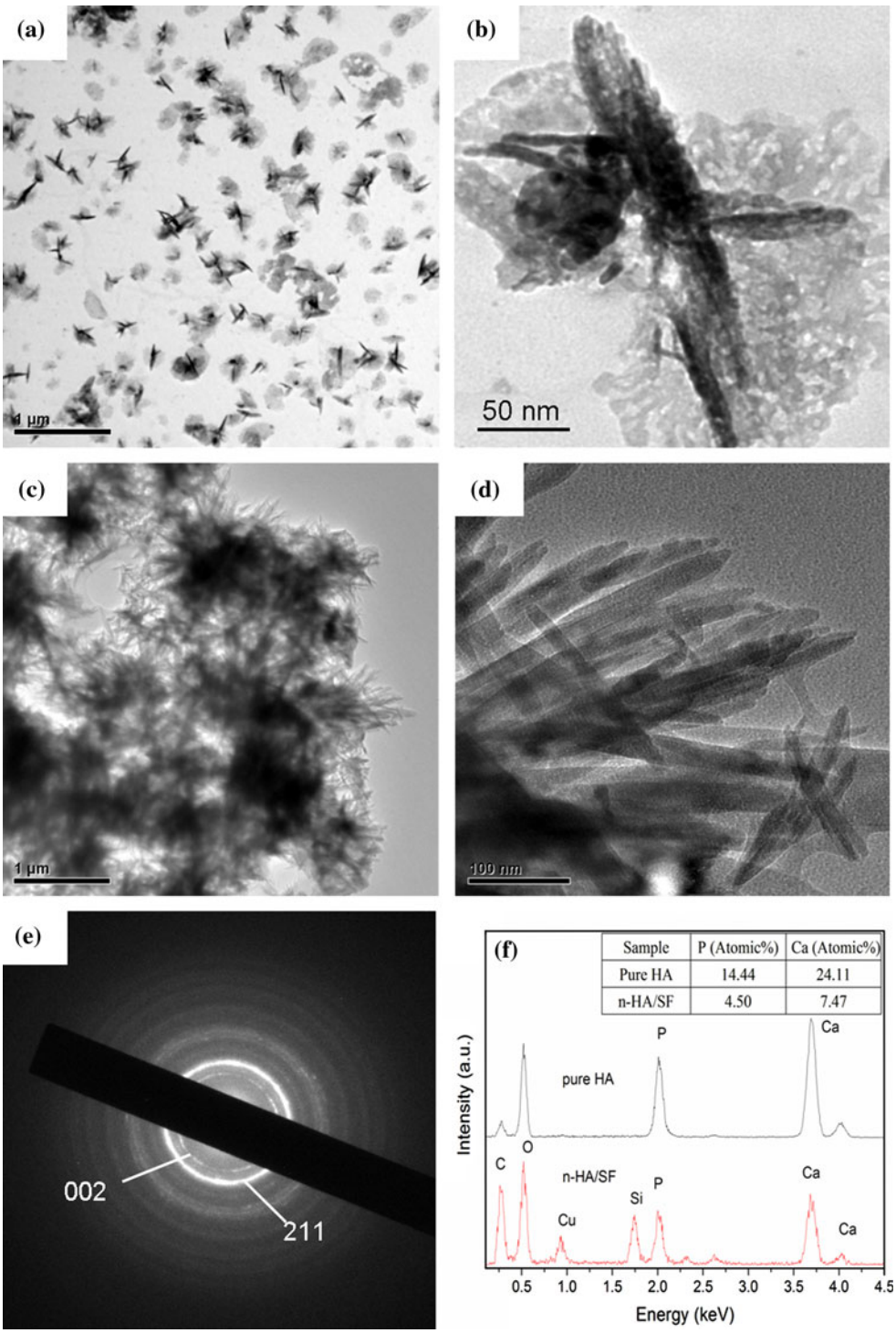

Fig. 2 **a**, **b** TEM images of pure HA; **c**, **d** TEM images of n-HA/SF composite; **e** the selected area electron diffraction (SAED) patterns of n-HA/SF; **f** EDS spectra of pure HA and n-HA/SF composite

(Ca/P = 24.11/14.44 = 1.67). These findings demonstrate that the fibroin proteins play an important role in regulating the nucleation and growth of the n-HA minerals.

Furthermore, the effects of SF for the HA minerals could be confirmed by the diversities of the sizes and shapes of the two samples. The precipitated HA crystals without fibroin proteins are much smaller in length–diameter ratio than those with the fibroin proteins. It is reasonable to view that the fibroin proteins regulate the self-organized process forming n-HA/SF composite.

As shown in Fig. 3, n-HA/SF composite and pure HA posses similar XRD patterns. All the diffraction peaks are well defined and assigned to crystalline HA, since no peaks from other calcium phosphate phases are detected.

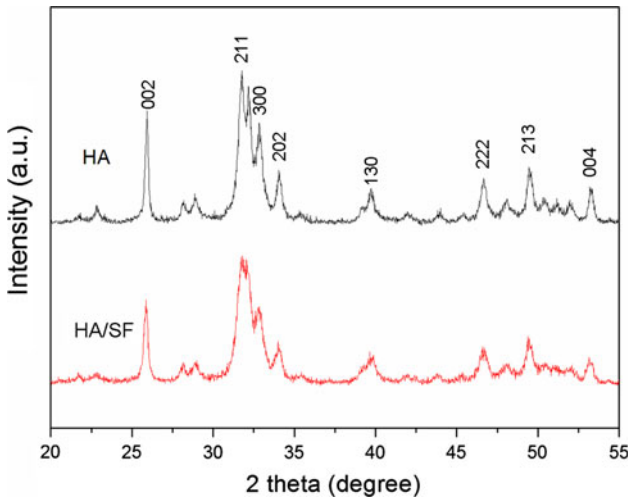

Fig. 3 XRD patterns of pure HA and n-HA/SF composite

It reveals that the involvement of SF does not change crystallographic structure of HA in the composite. Compared with the standard high temperature-sintered HA, the two samples present notable line broadening and overlap in terms of peaks, indicating that the obtained HA crystals have low crystallinity similar to the natural bone mineral [20, 21]. The poor crystalline nature of as-synthesized HA is possibly attributed to the low temperature procedure where the two samples were not subjected to sintering.

FT-IR spectroscopy is a good tool for structural investigations owing to the knowledge of the vibration origins of the functional groups. Figures 4 and 5 show a typical FT-IR spectrum of the n-HA/SF composite in the different frequency range, respectively. For a better comparison, FT-IR spectra of pure HA and SF were also added to the two figures. As shown in Fig. 4, the adsorption bands at 1095, 1033, 962, 604, and 564 cm^{-1} of n-HA/SF are nearly identical with those of pure HA. These bands can be assigned to molecular vibrations of the phosphate moiety in different chemical environments. The bands at 1449, 1415, and 876 cm^{-1} are derived from carbonate ions, which indicate that PO_4^{3-} sites in n-HA/SF are replaced partially by carbonate ions. It is well known that even if a carbonate-free solution is used [22], the carbonate ions can be incorporated into apatite stem from atmosphere carbon dioxide while dissolving, stirring, and reaction process. Therefore, the HA crystals formed on the SF templates were indentified as carbonate-containing HA. In Fig. 5, the adsorption bands at 1654, 1534, and 1239 cm^{-1} are ascribed to molecular vibration of the amide I, amide II, and amide III of pure SF, respectively. Compared with the spectrum of pure SF, these amide bands can also be detected from n-HA/SF composite correspondingly. However, the positions of these amide peaks are different and notable peak shifts (red shift) can easily be observed. Especially, the amide I (C=O) peak of n-HA/SF composite decreased to 18 cm^{-1}, shifted to 1626 cm^{-1}. The red shift proves that the strong chemical interaction exists between n-HA and SF, most probably between calcium ions of n-HA and amide groups of SF.

The TGA curves of pure HA, SF, and n-HA/SF composite are shown in Fig. 6. From TGA curve of pure HA, there is almost no notable weight loss occurred in the range from 50°−750°, indicating that the precipitated HA is thermally stable at high temperature. It can be seen from the TGA curve of n-HA/SF composite that the sample weight decreases with temperature increasing, especially in the ranges from 50°−120° assigned to the evaporation of water, and 350°−650° ascribed to the thermal decomposition of organic macromolecules. There is no change

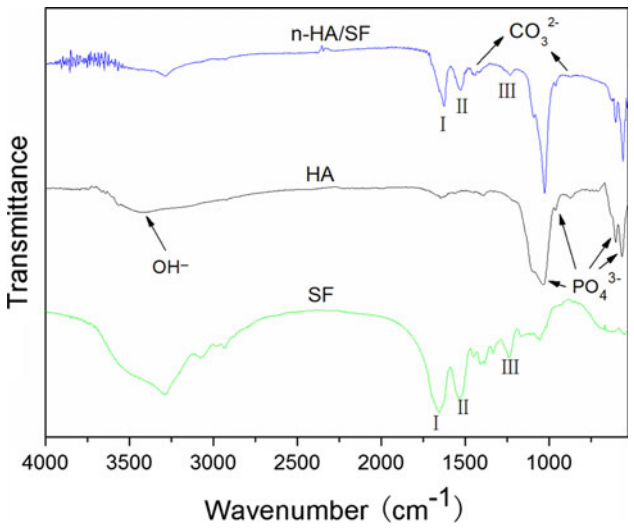

Fig. 4 FT-IR spectra of pure HA, SF and n-HA/SF composite in the frequency range of 500–4000 cm^{-1}

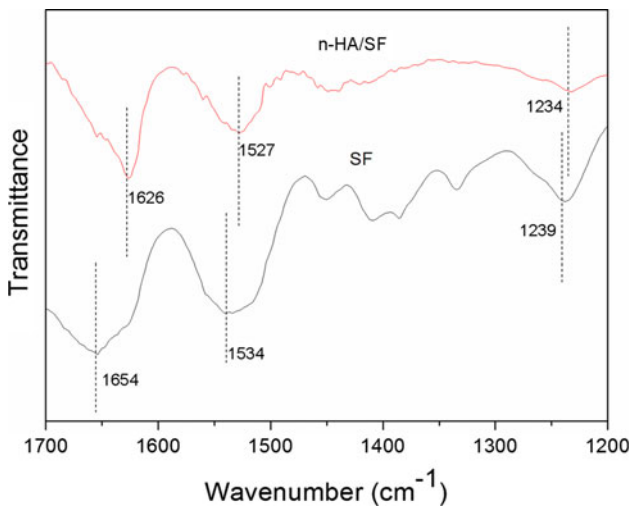

Fig. 5 FT-IR spectra of SF and n-HA/SF composite in the frequency range of 1200–1700 cm^{-1}

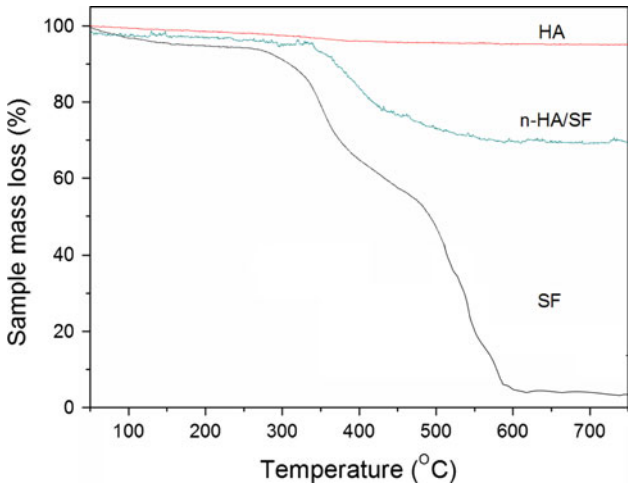

Fig. 6 TGA curves of pure HA, SF, and n-HA/SF composite

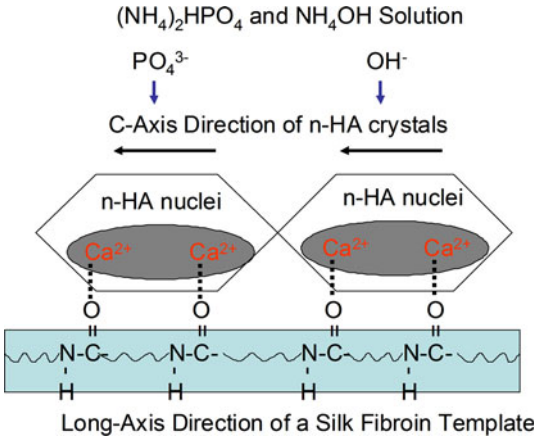

Fig. 7 Schematic illustration for the crystallochemical specific nucleation and growth of the n-HA crystals on the SF template

found in the weight of the composite above 650°, indicating that the organic contents are decomposed completely at 650°. The total weight loss for n-HA/SF composite is about 32%. From the TGA curve of SF, almost all the SF has been decomposed at 650°. It is clear that the 32% weight loss in n-HA/SF TGA curve should have origin from the thermal decomposition of SF in the composite. Therefore, the organic/inorganic weight ratio except water content for the composite is determined to be 28.9/71.1, almost consistent with the theoretical yield weight ratio of SF/HA. The thermal analysis reveals that SF molecules have been well incorporated into the composite.

It should be noted that, comparing with the TGA curves of SF and n-HA/SF composite, the initial decomposition temperature of the composite (about 360 °C) is far higher than that of SF (about 318 °C). The decomposition of SF is interesting, thought to be due to its different molecular environment. In the composite, the SF was strongly bounded with HA, and the molecular orientation and/or the crystallinity of SF were improved by the HA formation during the composite fabrication. Therefore, the initial decomposition temperature of n-HA/SF composite was improved.

It is well known that hydroxyl, carboxyl, and carbonyl groups have influences on inducing the self-organized orientation of HA crystals [6, 23, 24]. SF is linear polypeptide comprising 17 amino acids, whose main chain has abundant carbonyl groups, providing potential sites to bind with calcium ions. In this study, the red shifts of amide I, II, and III peaks in FT-IR analysis have supported the interactions between the HA crystals and the carbonyl groups in SF. Based on the results and discussion above, the formation process of n-HA/SF composite is proposed, as shown in Fig. 7.

In the $CaCl_2$ aqueous/ethanol solution, SF fibers can be easily dissolved and give more free carbonyl sites. Thus, calcium ions will bind with these carbonyl sites of SF to form calcium–SF complexes. When $(NH_4)_2HPO_4$ and NH_4OH solution are dropped into the above reaction system, PO_4^{3-} ions will accumulate at the calcium–SF complex sites and grow to tiny crystalline nuclei due to the supersaturation effects. After the nucleation, the growth of HA nanocrystal will be initiated from these active nucleation sites. Due to the strong chemical interactions between calcium ion and carbonyl groups of SF template, the SF will induce self-organized orientation of HA nanocrystal. Thus, the growth of HA crystal will progress spontaneously with preferred orientation (along its *c*-axis).

Conclusions

Nano-scaled HA-SF composite was fabricated via a simplified coprecipitation method with SF serving as a regulating template. Characterization results show that the inorganic component in the composite is poorly crystalline HA containing carbonate ions. The typical HA crystallites possess 200–500 nm in length and around 20–30 nm in width. The SF is incorporated into the composite by strong chemical interactions between HA and SF, probably take place via the chemical bonding between calcium ions and the carbonyl groups of SF. The strong chemical interaction results in the red shifts of amine groups in FT-IR analysis and the increase of initial decomposition temperature in TGA analysis. These findings suggest that the simplified coprecipitation method is a facile route to obtain good n-HA/SF composite, which could greatly save much time to bulk production of n-HA/SF composite as a promising biomaterial for bone ingrowth implant fixation.

Acknowledgements This work was sponsored by the National Key Basic Research Program of China (Grant No. 2009CB930000) and the Nanotechnology Program of Shanghai Science & Technology Committee, Shanghai (Grant No. 0852nm03100).

References

1. Du C, Cui FZ, Zhang W, Feng QL, Zhu XD, De Groot K (2000) J Biomed Mater Res A 50:518
2. Kikuchi M, Itoh S, Ichinose S, Shinomiya K, Tanaka J (2001) Biomaterials 22:1705
3. Mann S, Ozin GA (1996) Nature 365:499
4. Stupp SI, Braun PV (1997) Science 277:1242
5. Muthukumar M, Ober CK, Thomas EL (1997) Science 277:1225
6. Chang MC, Ko CC, Douglas WH (2003) Biomaterials 24:2853
7. Zhang YZ, Venugopal JR, El-Turki A, Ramakrishna S, Su B, Lim CT (2008) Biomaterials 29:4314
8. Hu QL, Li BQ, Wang M, Shen JC (2004) Biomaterials 25:779
9. Zhang L, Li YB, Yang AP, Peng XL, Wang XJ, Zhang X (2005) J Mater Sci Mater Med 16:213
10. Turco G, Marsich E, Bellomo F, Semeraro S, Donati I, Brun F, Grandolfo M, Accardo A, Paoletti S (2009) Biomacromolecules 10:1575
11. Kasuga T, Ota Y, Nogami M, Abe Y (2001) Biomaterials 22:19
12. Douglas T, Pamula E, Hauk D, Wiltfang J, Sivananthan S, Sherry E, Warnke PH (2009) J Mater Sci Mater Med 20:1909
13. Wei J, Li YB, Chen WQ, Zuo Y (2003) J Mater Sci 38:3303. doi: 10.1023/A:1025194122977
14. Nemoto R, Wang L, Aoshima M, Senna M, Ikoma T, Tanaka J (2004) J Am Ceram Soc 87:1014
15. Li YC, Cai YR, Kong XD, Yao JM (2008) Appl Surf Sci 255:1681
16. Du CL, Jin J, Li YC, Kong XD, Wei KM, Yao JM (2009) Mater Sci Eng C 29:62
17. Korematsu A, Furuzono T, Yasuda S, Tanaka J, Kishida A (2004) J Mater Sci 39:3221. doi:10.1023/B:JMSC.0000025865.44900.74
18. Takeuchi A, Ohtsuki C, Miyazaki T, Ogata S, Tanihara M, Tanaka H, Furutani Y, Kinoshita H (2003) Key Eng Mater 31:240
19. Wang L, Nemoto R, Senna M (2004) J Eur Ceram Soc 24:2707
20. Murugan R, Ramakrishna S (2004) Biomaterials 25:3829
21. Rhee SH, Tanaka J (2002) J Mater Sci Mater Med 13:597
22. Cao M, Wang Y, Guo C, Qi Y, Hu C (2004) Langmuir 20:4784
23. Zhang W, Liao SS, Cui FZ (2003) Chem. Mater 15:3221
24. Ethirajan A, Ziener U, Landfester K (2009) Chem Mater 21:2218